Plant Systematics and Evolution (2021) 307:26
https://doi.org/10.1007/s00606-021-01750-7

ORIGINAL ARTICLE

The highly conserved *rps*12 gene in ferns provides strong evidence for decreased substitution rates in the inverted repeat region

Jingyao Ping[1] · Aimin Li[2] · Peipei Feng[1] · Ming Zhu[1] · Yingjuan Su[3,4] · Ting Wang[1]

Received: 4 August 2020 / Accepted: 1 March 2021 / Published online: 19 March 2021

Abstract

The typical chloroplast genome consists of two inverted repeat (IR) and two single-copy (SC) regions. Each region has its own pattern of molecular evolution. Many studies have shown that the IR region has a low substitution rate. The plastid *rps*12 gene encodes ribosomal protein small subunit 12, which is composed of 5′-*rps*12 (exon 1) and 3′-*rps*12 (exon 2–3); 3′-*rps*12 is near the IR region and enters or leaves the IR region as it expands and contracts, enabling study of the variation in its substitution rate. We analyzed the evolutionary rate and adaptive evolution of the *rps*12 genes of 118 ferns and 2 lycophytes in a phylogenetic context using the maximum likelihood method. We found that the substitution rate of exon 2–3 was significantly lower in the IR region than in the LSC (1–11 times higher in the LSC), and also lower than that of exon 1 in the LSC region (1.9–6.7 times higher for exon 1). In addition, there was more GC content at the third codon position, and the *rps*12 gene encoded 123 amino acids, with 107 negative selection sites and 4 positive selection sites. These results prove that the substitution rate decreases after the sequence fragments enter the IR region and demonstrate the highly conserved nature of the *rps*12 gene.

Keywords Adaptive evolution · Ferns · GC content · Inverted repeat region · *Rps*12 · Substitution rates

Introduction

Chloroplast genomes in most plants consist of two inverted repeat (IR) regions. The large single-copy (LSC) region and the small single-copy (SSC) region. In most non-seed plant lineages, the IR region is 10-15 kb in size and generally contains four rRNA genes and five tRNA genes (Zhu et al. 2016). In ferns, some genes enter or leave the IR region with expansion and contraction of the region, including *rps*7, *psb*A, 3′-*rps*12, *ycf*2, *ndh*B (Li et al. 2016). The *rps*12 gene is very special, it encodes ribosomal protein small subunit 12 and consists of 5′-*rps*12 and 3′-*rps*12. Interestingly, the two parts are located a distance that is as far as half the size of the chloroplast genome (~70 kb) apart: 5′-*rps*12 contains only exon 1 and is located in the LSC region, while 3′-*rps*12 usually contains exon 2, introns and exon 3 and is located in the IR region. Some fern lineages have lost introns or 3′-rps12 enters the LSC region. During translation of *rps*12 gene, trans-splicing occurs between the 5′-*rps*12 and 3′-*rps*12 transcripts (Norihiro et al. 1987).

Different lineages and different genomes have different molecular evolutionary rates (Bromham and Penny 2003). Changes in the rate are often related to biological characteristics or population size. IR region may differ from the SC region in evolutionary rates due to its double-copy nature. Some studies have shown that genes in the IR region have lower substitution rates. In angiosperms, the IR region has lower synonymous and non-synonymous substitution rates than the SC region (Maier et al. 1995; Wolfe et al. 1987). Similarly, a low substitution rate has been found in the IR region in *Cycas revoluta* (Wu and Chaw 2015). In

Handling Editor: Yunpeng Zhao.

✉ Yingjuan Su
suyj@mail.sysu.edu.cn

✉ Ting Wang
tingwang@scau.edu.cn

[1] College of Life Sciences, South China Agricultural University, Guangzhou, China

[2] College of Education Sciences, Huaihua University, Huaihua, China

[3] School of Life Sciences, Sun Yat-Sen University, Guangzhou, China

[4] Research Institute of Sun Yat-Sen University in Shenzhen, Shenzhen, China

Leguminosae with loss of IR region, genes originally located in the IR region have synonymous substitution rates similar to those in the SC region (Perry and Wolfe 2002). Genes in the SC region were recently found to have substitution rates 3.7 times those of genes in the IR region. After a gene is transferred from the SC region to the IR region or vice versa, the substitution rates are consistent with other genes in the host region (Zhu et al. 2016). Gene translocation into the plastid IR region shows lower substitution rates and higher GC content (Li et al. 2016). However, the *Ginkgo biloba* *ycf*2 gene does not have a higher substitution rate after entering the SC region from the IR region (Lin et al. 2012). Note that some previous studies have ignored some of the interfering factors by comparing different genes or the same genes between different plants. Different genes have different biological functions and evolve in fundamentally different ways. Different species also experience different selection pressures. It is necessary to eliminate these factors to reach more accurate conclusions. Therefore, the *rps*12 gene with its special structure provides a natural condition for studying the change in substitution rate after the gene enters the IR region by comparing differences in evolution rate between the coding sequences in its two parts.

Ferns are the second largest group of vascular plants, with an estimated 10,578 extant species (PPG I 2016). With the development of next-generation sequencing, it is relatively easy to obtain sequences. This study examined 118 ferns and 2 lycophytes species and calculated the evolutionary rates of the *rps*12 codons to investigate the change in gene substitution rate after entering the IR region. We also assessed the selection process this particular gene has experienced in the evolution of ferns using selection pressure and adaptive evolution analyses.

Materials and methods

DNA extraction and sequencing sections have been removed.

Sequence data

We downloaded the complete chloroplast genome sequences of 120 plants (118 ferns and 2 lycophytes) from NCBI (Online Resource 1) and imported the sequences into Geneious Prime 2019.0.4 (Kearse et al. 2012) to extract the *rbc*L, *mat*K and *rps*12 genes. In addition, the coding sequence (*rps*12-CDS), exon 1, exon 2 and exon 3 (exon 2–3) of *rps*12 were extracted. The sequences were aligned and manually corrected using the ClustalW or ClustalW (codons) module in MEGA7.0 (Kumar et al. 2016), and stored as electronic supplementary material (Online Resource 2–6).

Relative GC content

The relative GC content at each position of the *rps*12 codon in each plant was calculated. That is, the ratio of GC content at each position of *rps*12 codon to the GC content of plastids genome of corresponding species, so as to reduce the influence caused by the difference in GC content of chloroplast genome between species. Significance was analyzed using two-tailed *t*-tests.

Construct phylogenetic trees

Based on the complete chloroplast genome and the tandem data set of *rbc*L and *mat*K (Hollingsworth et al. 2011; Li et al. 2016), two maximum likelihood trees were constructed using RaxmlGUI2 (GTRGAMMAI model and 100 Boostraps) (Stamatakis 2014) and MEGA 7.0 (GTR + G + I model and 1000 bootstraps), respectively. As the phylogenetic position of some fern groups is controversial, when determining the final tree, the Pteridophyte Phylogeny Group (PPG) I system was referred to at the order and family levels (PPG I 2016). The phylogenetic relationships of genera and species were determined from the two constructed trees.

Calculate the rate of evolution and hypothesis test

The rate of evolution was calculated using HyPhy 2.2.4 (Pond et al. 2005) with the partition type set to nucleotide, the HKY85 substitution model and local parameters; the transition (*trst*) and transversion (*trsv*) rates and ratio (*trsv*/*trst*) were calculated. The synonymous (d*S*) and non-synonymous (d*N*) substitution rates and *ω* (d*N*/d*S*) were calculated using the codon partition type, MG94 × HKY85_3 × 4 substitution model and local parameters. For the codon type, the substitution mode (MG94 × HKY85 × 3_4 × 2_rate), parameters (rate Het.) and rate classes (4) were used to analyze selective pressure. The Wilcoxon rank-sum test and Mann–Whitney *U*-test were performed with IBM SPSS Statistics 22.0.

The hypothesis test first saves the original data as a full model, then constrains the exon 1 value of each species branch to equal exon 2–3 and saves it as a null model after optimization, before finally performing a likelihood ratio test. Hypothesis testing was mainly used to test for significant difference in the evolutionary rate between exon 1 and exon 2–3.

Identification of positive amino acid sites and alignment of amino acid sequences

The positive amino acid selection sites of the *rps*12 gene were identified using codeml in the PAML 4.9 package

(Yang 2007). Three models were used to calculate the number of parameters and likelihood values and estimate the value of the parameters and positively selected sites: the branch, site and branch-site models. The Chi-square test was performed using chi2.exe. The two-ratio model (Model2) in the branch model was used to calculate the ω values of the foreground branch and background branches.

To understand the *rps*12 sequence characteristics, we added *rps*12 amino acid sequences from six species (Table 1) and aligned 126 amino acid sequences using MEGA7.0. Finally, the online SWISS-MODEL tool was used to predict the structure of RPS12 protein (https://www.swissmodel.expasy.org/).

Results

Characteristics of *rps*12 gene

The size of the *rps*12 gene ranges from 372 (no introns) to 985 bp (*Pteris vittata*). The *rps*12 coding sequence in all species is the same size, 372 bp, and is divided into three exons: exon 1 is 114 bp, exon 2 is 232 bp, and exon 3 is 26 bp. In all, 106 plants also had introns which ranged in size from 447 to 613 bp. Figure 1 shows the phylogenetic tree of the 120 species; according to the location of exon 2–3, its divided into two groups: in the IR region (IR-109) and in the LSC region (LSC-11). Figure 2 shows the double-tailed *t*-test results of the relative GC content. The mean relative GC content in the first and second codon positions was lower in IR-109 than in LSC-11 ($P_{\text{first}} = 0.658$ $P_{\text{second}} = 0.032$), while the relative content in the third codon position of the *rps12* gene was higher ($P_{\text{third}} = 0$).

Phylogenetic relationships of ferns

The phylogenetic relationships of the complete chloroplast genome construction are chaotic (Online Resource 7). The base group of ferns (Equisetales, Ophioglossales and Schizaeales) did not form a monophyletic branch. Lindsaeaceae and *Saccoloma inaequale* and *Neocheiropteris palmatopedata* in Polypodiales are located at the base of ferns. In the tree constructed with the concatenated data set (*rbc*L and *mat*K) shows that the phylogenetic relationships among the various groups are relatively clear (Online Resource 8): the basal group forms a monophyletic branch, Equisetales and Marattiales have low bootstrap support, and Salviniales and Cyathales as well as *Diplopterygium glaucum* and Hymenophyllales are sister groups. In two trees, Polypodiales, Rhachidosoraceae, Cystopteridaceae, Dennstaedtiaceae, Lindsaeaceae and Saccolomataceae have uncertain positions. We referred to the PPG I system at the order and family levels, and manually adjusted the tree to obtain the final phylogenetic tree for analyses of evolutionary rates (Fig. 1).

Analysis of the rate of evolution

For IR-109, it can be intuitively observed numerically that 80% (for *trst*), 94% (for *trsv*), 94% (for *ratio*), 84% (for d*N*), 76% (for d*S*) and 86% (for ω) of the species branches had exon 1 values greater than or equal to exon 2–3 values (Online Resource 9). The parameter mean value of exon 1 was 1.9–6.7 times that of exon 2–3, and there were significant differences, except in *ratio* ($P = 0.05$) (Fig. 3a). For LSC-11, only *trst* was significantly different ($P = 0.028$) and exon 2–3 had twice the value of exon 1 (Fig. 3b).

For exon 1, the mean value in IR-109 was lower than in LSC-11, and there were significant differences in *trsv* and *ratio* (Fig. 4a). For exon 2–3, the mean value of LSC-11 was 1–11 times that of IR-109, and the difference was significant (Fig. 4b). For *rps*12-CDS, the mean value of LSC-11 (except ω, $P = 0.893$) was 1.6–6 times that of IR-109, with a significant difference (Fig. 4c).

The results of hypothesis testing are shown in Fig. 5. For all four parameters, more than 80% of the branches of species that could be effectively constrained were acceptable for hypothesis testing.

Selection pressure and Identification of positively selected amino acid sites

With HyPhy, setting the Bayes factor value as greater than 20, we detected 2 positively selected sites (17G, 74L) and 107 negatively selected sites (Fig. 6).

Table 1 Information on six species used for amino acid sequence alignment

	Order	Family	Species name	NCBI Accession number
Bacteria	Enterobacterales	Enterobacteriaceae	*Escherichia coli FVEC141*	EFE98771
liverwort	Marchantiales	Marchantiaceae	*Marchantia polymorpha*	AZU95199
gymnosperm	Cycadales	Cycadaceae	*Cycas revoluta*	YP_007474599
angiosperm	Solanales	Solanaceae	*Nicotiana tabacum*	AMM05616
angiosperm	Fabales	Fabaceae	*Acacia xanthina*	CUR08185
angiosperm	Fabales	Fabaceae	*Pisum fulvum*	AUM82294

Fig. 1 Phylogenetic tree. The blue species names represent *rps*12 located in the IR region (IR-109), and the green species names represent *rps*12 located in the LSC region (LSC-11)

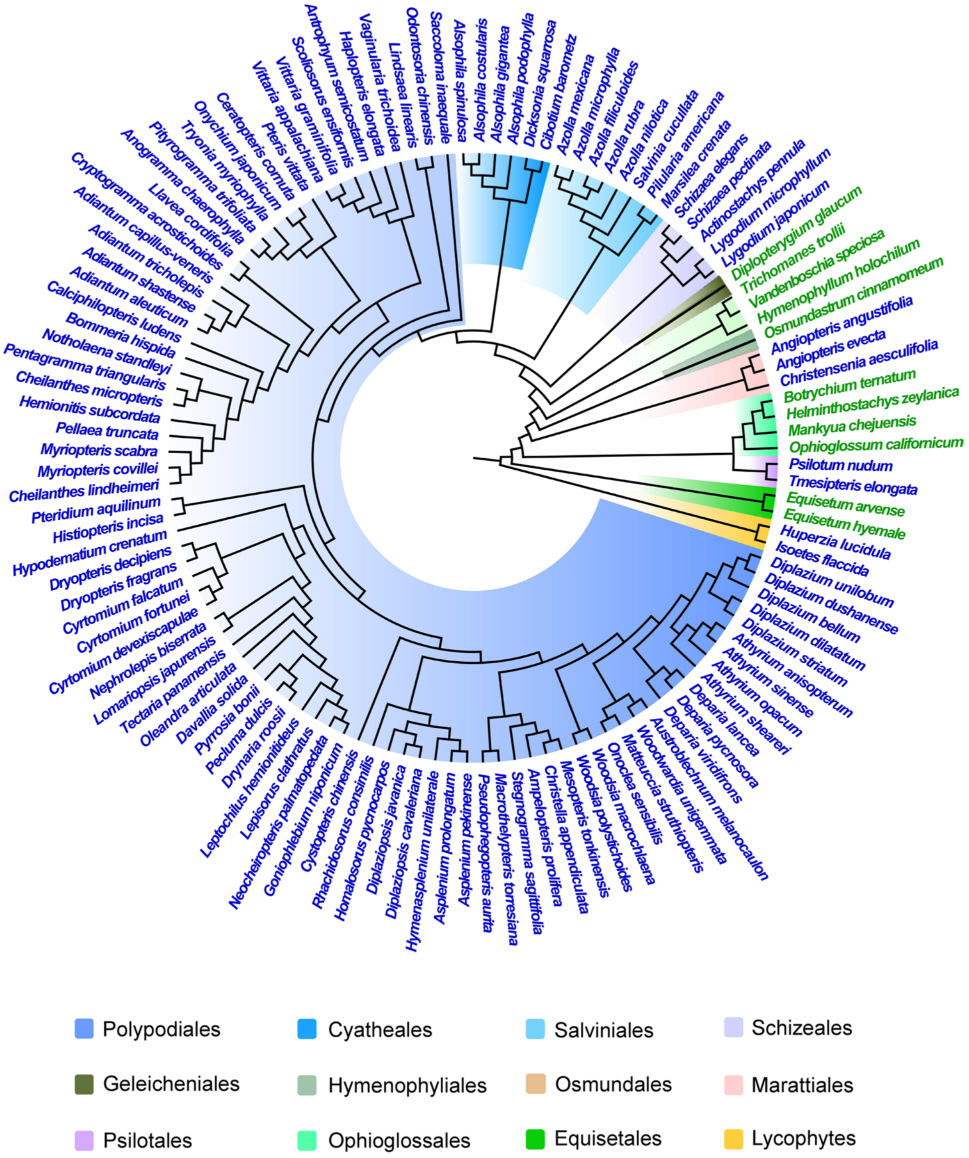

Fig. 2 Relative GC content of content. *$P = 0$. Note that the third position of the codon has a higher relative GC content of IR-109 than LSC-11

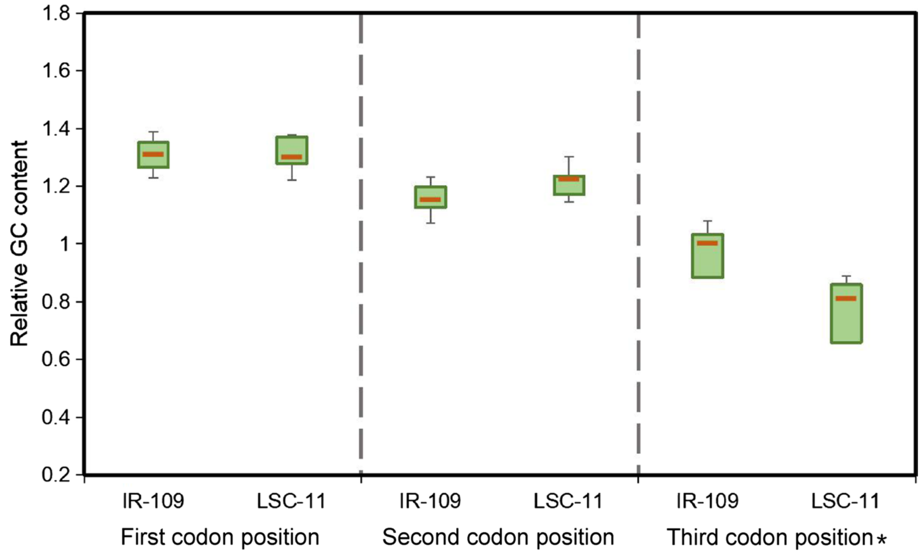

Fig. 3 Significance analysis of the mean substitution rates of exon 1 and exon 2–3 in IR-109 and LSC-11. **a** IR-109. **b** LSC-11

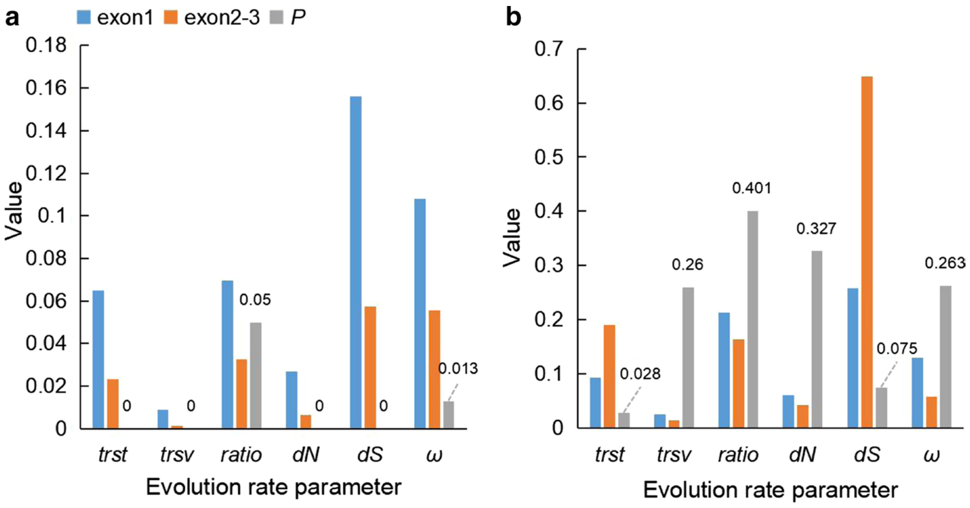

Fig. 4 Significance analysis of mean substitution rates of IR-109 and LSC-11 in three data sets. **a** exon 1. **b** exon 2–3. **c** *rps*12-CDS

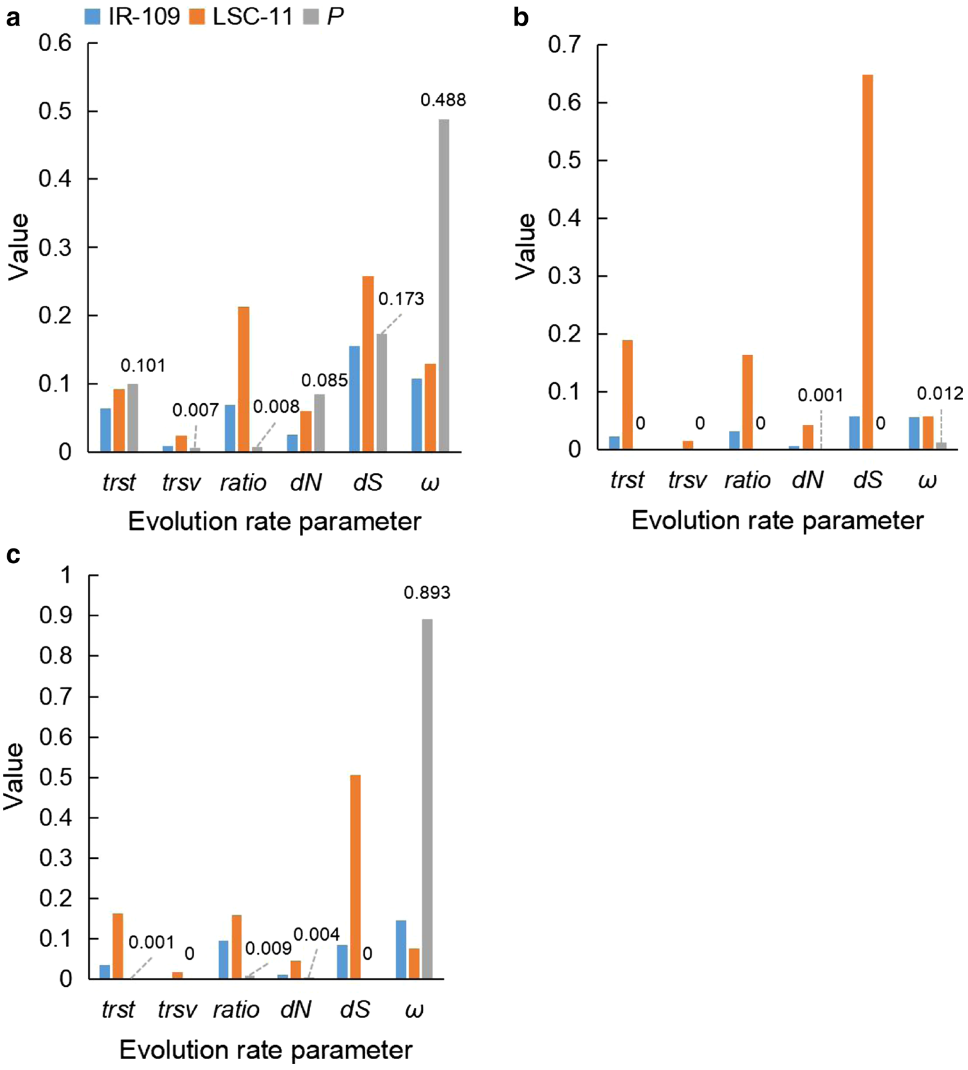

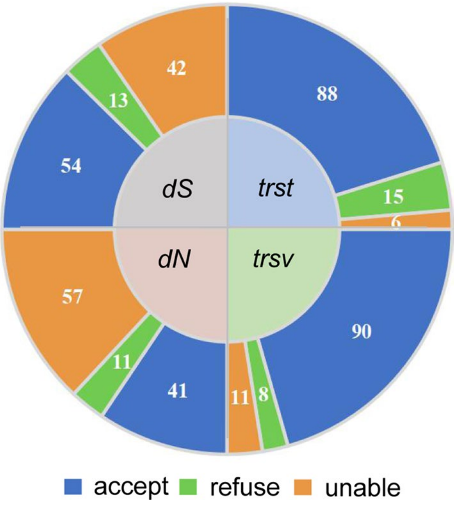

Fig. 5 Hypothesis testing. Set the original data as an alternative hypothesis, and the null hypothesis is to constrain the value of exon2-3 to be equal to exon1 and perform the likelihood ratio test of the two hypotheses. accept: $P > 0.05$. refuse: $P < 0.05$. unable: the number of the species branches that cannot be effectively constrained by assumptions. The number represents the number of branches of a species

In the branch model, the F model detected 50 branches with $\omega > 1$: these were used as foreground branches in the branch-site model. In Model2, for three different sequence sets (*rps*12-CDS, exon 1 and exon 2–3), the likelihood ratio test results of the foreground (LSC-11) and background branches (IR-109) were calculated. The results for M0 and Model2 showed that ω_1 of exon 2–3 was 3.3 times that of ω_2 ($P = 0$). In the site model, the likelihood ratio tests between the four pairs of models differed significantly. The results of M1a-M2a were taken as the standard and a posterior probability greater than 0.95 is taken as the condition to identify three positively selected amino acid sites (14Q, 16G, 74L). The likelihood ratio test of the branch-site model, null and alternative was significantly different ($P = 0.031$), and no positive selective amino acid sites were identified when the posterior probability was greater than 0.95 (Tables 2 and 3).

Amino acid sequence alignment

The amino acid sequences of *rps*12 from 126 plants were aligned, and the protein structure was predicted using the *rps*12 amino acid sequence of *Drynaria roosii* as a reference. As shown in Fig. 6, there were 57 completely consistent sites, all of which experienced negative selection. The predicted protein structure detected negative selection in 38 of the 44 sites in the α-helix and β-sheet regions, and 4 positive selection sites (14Q, 16G, 17G and 74L) in the loop or irregular region.

Discussions

Decreased substitution rates

Consistent with previous studies (Li et al. 2016), the gene substitution rates decreased after entering the IR region.

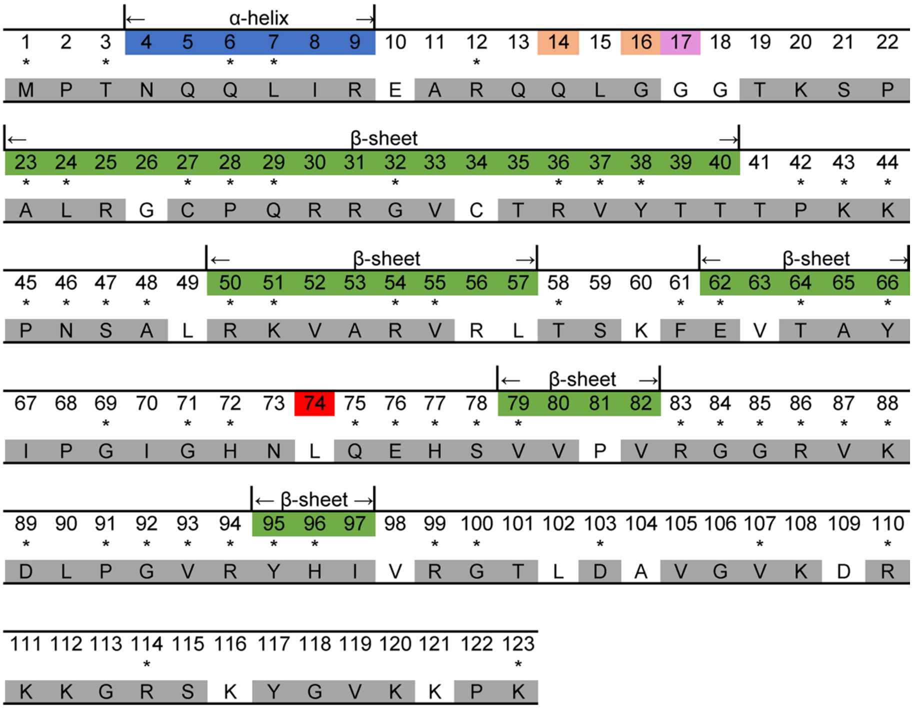

1	2	3	4	5	6	7	8	9	10	11	12	13	14	15	16	17	18	19	20	21	22
*		*			*	*					*										
M	P	T	N	Q	Q	L	I	R	E	A	R	Q	Q	L	G	G	G	T	K	S	P
23	24	25	26	27	28	29	30	31	32	33	34	35	36	37	38	39	40	41	42	43	44
*	*			*	*	*			*				*	*	*				*	*	*
A	L	R	G	C	P	Q	R	R	G	V	C	T	R	V	Y	T	T	T	P	K	K
45	46	47	48	49	50	51	52	53	54	55	56	57	58	59	60	61	62	63	64	65	66
*	*	*	*		*	*			*	*			*			*	*		*		*
P	N	S	A	L	R	K	V	A	R	V	R	L	T	S	K	F	E	V	T	A	Y
67	68	69	70	71	72	73	74	75	76	77	78	79	80	81	82	83	84	85	86	87	88
		*		*	*			*	*	*	*	*				*	*	*	*	*	*
I	P	G	I	G	H	N	L	Q	E	H	S	V	V	P	V	R	G	G	R	V	K
89	90	91	92	93	94	95	96	97	98	99	100	101	102	103	104	105	106	107	108	109	110
*		*	*	*	*	*	*			*	*			*				*			*
D	L	P	G	V	R	Y	H	I	V	R	G	T	L	D	A	V	G	V	K	D	R
111	112	113	114	115	116	117	118	119	120	121	122	123									
			*									*									
K	K	G	R	S	K	Y	G	V	K	K	P	K									

Fig. 6 Amino acid sequence alignment (with *Drynaria roosii* as the reference sequence). The number 1–123 indicates the amino acid site number. Blue area indicates the sites located in the α-helix region. Green area indicates the sites located in the β-sheet region. "*" represents the consistent sites of 126 amino acid sequence alignment. With Hyphy, under the condition that the Bayes factor is greater than 20, 2 positive selection sites (pink area-17 and red area-74) and 107 negative selection sites (gray area) are screened out. Three positive selective amino acid sites (red area-74, aurantium area 16 and 14) were identified using PAML with a posterior probability of $P > 0.95$

Table 2 Parameter estimates and log-likelihood value under model

Model	Number of parameters	l	Estimated value of parameters	Positively selectively sites
Branch model				None
*rps*12-CDS				
M0 (One ratio)	240	– 5701.207	$\omega=0.105$	
F (Free ratio)	477	– 5607.925	$\omega_1=33.696$, $\omega_2=999$, $\omega_3 \ldots \omega_{50}$	
Model2 (Two ratio)	241	– 5699.622	$\omega_1=0.110$, $\omega_2=0.068$	
exon 1				
M0	240	– 2492.048	$\omega=0.160$	
Model2	241	– 2491.450	$\omega_1=0.155$, $\omega_2=0.245$	
exon 2–3				
M0	240	– 3007.930	$\omega=0.067$	
Model2	241	– 2999.927	$\omega_1=0.076$, $\omega_2=0.023$	
Site model				
M1a (Near neutral)	241	– 5494.292	$p_0=0.880$, $\omega_0=0.120$ $p_1=0.035$, $\omega_1=1$	Not allowed
M2a (Positive selection)	243	– 5486.418	$p_0=0.879$, $\omega_0=0.036$ $p_1=0.098$, $\omega_1=1$ $p_2=0.024$, $\omega_2=2.371$	14 L*, 16 K**, 74 L*
M3 (Discrete)	244	– 5442.195	$p_0=0.765$, $\omega_0=0.012$ $p_1=0.19515$, $\omega_1=0.284$ $p_2=0.040$, $\omega_2=1.578$	14 L**, 16 K**, 17G**, 74 L**
M7 (beta)	241	– 5453.620	$p=0.114$, $q=0.604$	Not allowed
M8 (beta and ω)	243	– 5438.623	$p_0=0.975$, $p=0.159$ $\mathrm{q}=1.447$ $p_1=0.025$, $\omega=2.088$	14 L**, 16 K**, 74 L**
M8a (beta and $\omega=1$)	242	– 5447.008	$p_0=0.950$, $p=0.188$ $q=1.870$ $p_1=0.050$, $\omega=1$	Not allowed
Branch-site model				
Alternative Model A (ω_2 estimated)	243	– 5491.164	$p_0=0.819$, $p_1=0.113$ $p_{2a+2b}=0.068$, $\omega_2=9.532$	
Null Model A ($\omega_2=1$)	242	– 5493.490	$p_0=0.795$, $p_1=0.110$ $p_{2a+2b}=0.096$, $\omega_2=1$	Not allowed

*Posterior probability $P>95\%$

**Posterior probability $P>99\%$

When exon 2–3 enters the IR region, its substitution rate significantly decreased. The substitution rate of exon 1 was 1.9–6.7 times that of exon 2–3. Similarly, that of exon 2–3 in LSC was 1–9 times that in the IR region.

Because exon 1 and exon 2–3 encode RPS12 together, we tested whether the substitution rate of exon 1 may be affected by the decrease in the exon 2–3 substitution rate in the IR region. The results showed that *trsv* and *ratio* of exon 1 located in IR-109 were significantly decreased, but no differences consistent with exon 2–3 were seen. In a previous study of 70 species (IR-61 and LSC-9), we found that exon 1 of IR-61 had significantly lower *trsv* and *dN* compared to LSC-9. Perhaps conversions and non-synonymous substitutions readily lead to amino acid changes, so exon 1 and exon 2–3 have consistent conversion and non-synonymous substitution rates. Of course, the results may arise from the large difference in the amount of data in the IR-109 and LSC-11 groups. Nevertheless, the substitution rate of *rps*12-CDS of IR-109 was also significantly decreased, indicating that the substitution rate of the exon 2–3 sequence affected the substitution rate of the gene-coding sequence.

The low rate of evolution in IR may be due to its double-copy-related repair mechanism (Perry and Wolfe 2002). Biased gene transformation can occur throughout the genome; due to its double-copy nature, the frequency of gene transformation is relatively higher in the IR region, and

Table 3 Likelihood ratio statistics

	Comparison of models	$2\Delta l$	*df*	*P*
Branch model				
*rps*12-CDS	M0–Model2	3.169	1	0.075
	M0–F	186.564	237	0.993
exon 1	M0–Model2	1.195	1	0.274
exon 2–3	M0–Model2	16.005	1	0
Site model				
	M0–M3	516.825	4	0**
	M1a–M2a	15.749	2	0**
	M7–M8	29.994	2	0**
	M8–M8a	16.770	1	0**
Branch-site model				
	ModelA: Null—Alternative	4.650	1	0.031

*$P > 95\%$

**$P > 99\%$

gene transformation can also occur between the two copies in the IR region (Khakhlova and Bock 2006). As a result, only a small number of substitutions can be detected, so they show a lower rate of evolution.

Selection pressure affects the substitution rate and GC content increase

Previous research has suggested that protein-level selection has little or no effect on the rate decrease (Li et al. 2016). We reached different conclusions: selection pressure may influence the decreased substitution rate. Our calculations using HyPhy and the two-ratio model in the PAML branch model show that *rps*12-CDS and exon 1 both fit the M0 model, showing that the selection pressure experienced by IR-109 and LSC-11 is consistent. However, exon 2–3 fits Model2 ($P_{\text{M0-Model2}} = 0$), which indicates that exon 2–3 experiences different selection pressures on the LSC-11 ($\omega = 0.076$) and IR-109 ($\omega = 0.023$) branches. Therefore, in LSC-11, relaxed selection would tend to increase the number of nucleotide substitutions per unit time and cause higher nucleotide substitution rates. Compared to LSC-11, IR-109 experienced constrained selection pressure, coupled with the repair effects of gene conversion, and a lower substitution rate was detected.

Studies have shown that GC content is higher in the IR region than in the SC region. There are many A/T to G/C substitutions in the IR region of cycads (Wu and Chaw 2015). Li et al. (2016) found that the gene GC content increased after entering the IR region. We also found that after exon 2–3 entered the IR region, the GC content of the third codon position significantly increased, indicating that there is a GC bias for gene conversion.

Highly conservative characteristics

Lower substitution rates often indicate that a gene is relatively stable and highly conserved. The fern *rps*12 coding sequence is 372 bp and the size of the three exon sequences is also constant. At the amino acid level, 87% of the amino acid sites experienced strong negative selection, including 39 of the 44 sites in the α-helix and β-sheet domains, and most of the sites interacting with the S4, S8, 16 and S17 proteins. The four positive selection sites in the loop or irregular region have limited effects on the structure and function of the *rps*12 gene. From prokaryotes to angiosperms, the amino acid sequence has remained high consistent during evolution. All of these results demonstrate the highly conserved nature of the *rps*12 sequence. Corresponding to its conservative characteristics, exon 2–3 of the ferns and the ancestral lycophytes is located in the IR region, indicating that exon 2–3 is more inclined to be located in the IR region to maintain a lower substitution rate.

Conclusion

The results of this study of the *rps*12 gene provide strong evidence for decreased substitution rates and increased GC content when the gene is located in the IR region. The gene is highly conserved, providing a reference for understanding the structural changes and functional variation in the *rps*12 gene. The decreased substitution rates of gene sequences and relatively high conservation in the IR region seem to characterize the IR region. Study of the IR region provides insights into the basic characteristics of chloroplast genomes and the heterogeneity of substitution rates.

Information on electronic supplementary material

Online Resource 1. Plastomes sampled in this study.
Online Resource 2. Alignment of the complete chloroplast genome sequences used in this study.
Online Resource 3. Alignment of the tandem data set of *rbcL* and *matK* sequences used in this study.
Online Resource 4. Alignment of the *rps*12-CDS sequences used in this study.
Online Resource 5. Alignment of the exon1 sequences used in this study.
Online Resource 6. Alignment of the exon2-3 sequences used in this study.

Online Resource 7. Maximum likelihood (ML) tree constructed based on the complete chloroplast genome.
Online Resource 8. Maximum likelihood (ML) tree constructed based on concatenated data sets of *rbcL* and *matK*.
Online Resource 9. Distribution of exon 1 and exon 2-3 values for each species in IR-109.

Supplementary Information The online version contains supplementary material available at https://doi.org/10.1007/s00606-021-01750-7.

Acknowledgements The authors wish to thank Ziying Liang, and Xiuqin Ma for technical assistance and sharing opinions, ShanShan Liu for the sample. This work was funded by the National Natural Science Foundation of China (31670200, 31770587, 31872670 and 32071781).

Availability of data and material Data are available as Electronic Supplementary Material.

Declarations

Conflict of interest The authors declare that they have no conflict of interest.

References

Bromham L, Penny D (2003) The modern molecular clock. Nat Rev Genet 4:216–224. https://doi.org/10.1038/nrg1020

Hollingsworth PM, Graham SW, Little DP (2011) Choosing and using a plant DNA barcode. PLoS One 6:e19254. https://doi.org/10.1371/journal.pone.0019254

Kearse M, Moir R, Wilson A et al (2012) Geneious Basic: an integrated and extendable desktop software platform for the organization and analysis of sequence data. Bioinformatics 28:1647–1649. https://doi.org/10.1093/bioinformatics/bts199

Khakhlova O, Bock R (2006) Elimination of deleterious mutations in plastid genomes by gene conversion. Pl J 46:85–94. https://doi.org/10.1111/j.1365-313X.2006.02673.x

Kumar S, Stecher G, Tamura K (2016) MEGA7: molecular evolutionary genetics analysis version 7.0 for bigger datasets. Molec Biol Evol 33:1870–1874. https://doi.org/10.1093/molbev/msw054

Li FW, Kuo LY, Pryer KM, Rothfels CJ (2016) Genes translocated into the plastid inverted repeat show decelerated substitution rates and elevated GC content. Genome Biol Evol 8:2452–2458. https://doi.org/10.1093/gbe/evw167

Lin CP, Wu CS, Huang YY, Chaw SM (2012) The complete chloroplast genome of *Ginkgo biloba* reveals the mechanism of inverted repeat contraction. Genome Biol Evol 4:374–381. https://doi.org/10.1093/gbe/evs021

Lowe TM, Eddy SR (1997) tRNAscan-SE: a program for improved detection of transfer RNA genes in genomic sequence. Nucl Acids Res 25:955–964. https://doi.org/10.1093/nar/25.5.955

Maier RM, Neckermann K, Igloi GL et al (1995) Complete sequence of the maize chloroplast genome: gene content, hotspots of divergence and fine tuning of genetic information by transcript editing. J Molec Biol 251:614–628. https://doi.org/10.1006/jmbi.1995.0460

Norihiro Z, Keita T, Kazuo S et al (1987) Trans splicing in vivo: joining of transcripts from the 'divided' gene for ribosomal protein S12 in the chloroplasts. Febs J 210:153–156. https://doi.org/10.1016/0014-5793(87)81326-1

Perry AS, Wolfe KH (2002) Nucleotide substitution rates in legume chloroplast DNA depend on the presence of the inverted repeat. J Molec Evol 55:501–508. https://doi.org/10.1007/s00239-002-2333-y

Pond SL, Frost SD, Muse SV (2005) HyPhy: Hypothesis testing using phylogenies. Bioinformatics 21:676–679. https://doi.org/10.1093/bioinformatics/bti079

PPG I The Pteridophyte Phylogeny group, (2016) A community-derived classification for extant lycophytes and ferns. J Syst Evol 54:563–603. https://doi.org/10.1111/jse.12229

Stamatakis A (2014) RaxML version 8: a tool for phylogenetic analysis and post-analysis of large phylogeies. Bioinformatics 30:1312–1313. https://doi.org/10.1093/bioinformatics/btu033

Wolfe KH, Li WH, Sharp PM (1987) Rates of nucleotide substitution vary greatly among plant mitochondrial, chloroplast, and nuclear DNAs. Proc Natl Acad Sci USA 84:9054–9058. https://doi.org/10.1073/pnas.84.24.9054

Wu CS, Chaw SM (2015) Evolutionary stasis in Cycad plastomes and the first case of plastome GC-biased gene conversion. Genome Biol Evol 7:2000–2009. https://doi.org/10.1093/gbe/evv125

Wyman SK, Jansen RK, Boore JL (2004) Automatic annotation of organellar genomes with DOGMA. Bioinformatics 20:3252–3255. https://doi.org/10.1093/bioinformatics/bth352

Yang Z (2007) PAML 4: phylogenetic analysis by maximum likelihood. Molec Biol Evol 24:1586–1591. https://doi.org/10.1093/molbev/msm088

Zerbino DR, Birney E (2008) Velvet: algorithms for de novo short read assembly using de Bruijn graphs. Genome Res 18:821–829. https://doi.org/10.1101/gr.074492.107

Zhu AD, Guo WH, Gupta SS et al (2016) Evolutionary dynamics of the plastid inverted repeat: the effects of expansion, contraction, and loss on substitution rates. New Phytol 209:1747–1756. https://doi.org/10.1111/nph.13743